

# Resonance Raman Spectroscopic Detection of Steric-Induced Distortions of Axial Ligand Binding for Dioxygen Adducts of Superstructured Cobalt-Porphyrin Complexes

Leonard M. Proniewicz,<sup>1a,b</sup> Alan Bruha,<sup>1a</sup> Kazuo Nakamoto,<sup>\*,1a</sup> Yoshio Uemori,<sup>1c</sup> Eishin Kyuno,<sup>1c</sup> and James R. Kincaid<sup>\*,1a</sup>

*Contribution from the Department of Chemistry, Marquette University, Milwaukee, Wisconsin 53233, The Regional Laboratory of Physicochemical Analyses and Structural Research, Jagiellonian University, ul. Karasia 3, 30-060 Cracow, Poland, and Department of Pharmaceutical Science, School of Pharmacy, Hokuriku University, 3, Ho Kanagawa-Machi, Kanazawa 920-11, Japan. Received May 15, 1991*

**Abstract:** Resonance Raman studies are carried out for the O<sub>2</sub> adducts of superstructured "jellyfish" cobalt-porphyrin complexes with several trans-axial ligands, namely, pyridine, 3,5-lutidine, and imidazole as well as several of their deuteriated analogues. Two superstructured, bis-strapped porphyrins, having either short (9 carbon atoms) or long (12 carbon atoms) strap lengths, are employed along with sterically relaxed (non-strapped) porphyrins. It is found that the short-strap derivative induces distortion of the bound ligands while the long-strap analogue permits normal, unencumbered binding. While the distortion of the trans-axial ligand does not significantly affect the Co-O<sub>2</sub> linkage, as judged by the constancy of the inherent frequency of ν(O–O), significant shifts of the ligand internal modes give rise to substantially altered spectra as a result of variations in the strength of vibrational coupling of the ν(O–O) with internal modes of the trans-axial ligand.

## Introduction

Resonance Raman (RR) spectroscopy has been effectively employed to investigate the detailed structure and bonding for a large number of exogenous ligand adducts with a variety of heme proteins and their model compounds.<sup>2</sup> In a few cases, all of the internal modes associated with the Fe–XY fragment (ie., ν(Fe–X), δ(FeXY) and ν(X–Y)) are efficiently enhanced via resonance with accessible charge-transfer transitions. Very recently we have shown that all three vibrations associated with the FeO<sub>2</sub> molecular fragment can also be enhanced with 406.7-nm excitation in the case of five-coordinate Fe(por)O<sub>2</sub> formed in low-temperature O<sub>2</sub> matrices.<sup>3</sup> While the ν(O–O) of the O<sub>2</sub> adducts of the oxygen transport proteins, hemoglobin (Hb) and myoglobin (Mb), is not enhanced, Tsubaki and Yu<sup>4</sup> demonstrated that it is strongly enhanced by excitation near 400 nm in the case of their cobalt-substituted analogues.

A systematic study of the RR spectra of a series of O<sub>2</sub> adducts of cobalt-substituted porphyrins was undertaken in our laboratory in order to assess the factors that influence the vibrational behavior of bound dioxygen.<sup>5</sup> While these studies did permit an evaluation of the steric, electronic, and environmental factors which affect ν(O–O), they also revealed an inherent tendency for bound dioxygen to couple with internal modes of the trans-axial ligand and/or other solution components. Such effects give rise to frequency and intensity perturbations of the coupled modes and significant enhancements of (otherwise RR silent) axial ligand modes.

(1) (a) Marquette University. (b) Jagiellonian University. (c) Hokuriku University.

(2) (a) Yu, N. T.; Kerr, E. A. In *Biological Applications of Raman Spectroscopy*; Spiro, T. G., Ed.; Wiley-Interscience: New York, 1987; Vol. 3, p 39. (b) Spiro, T. G. In *Iron Porphyrins*; Lever, A. B. P., Gray, H. B., Eds.; Addison-Wesley: Reading, MA, 1983; Vol. 2, p 89. (c) Kitagawa, T.; Ozaki, Y. *Struct. Bonding* 1987, 64, 71.

(3) (a) Proniewicz, L. M.; Paeng, I. R.; Nakamoto, K. *Proceedings of the XII International Conference on Raman Spectroscopy*; Durig, J. R., Sullivan, J. Eds.; J. Wiley and Sons: New York, 1990; p 570. (b) Proniewicz, L. M.; Paeng, I. R.; Nakamoto, K. *J. Am. Chem. Soc.* 1991, 113, 3294.

(4) Tsubaki, M.; Yu, N. T. *Proc. Natl. Acad. Sci. U.S.A.* 1981, 78, 3581.

(5) (a) Bajdor, K.; Kincaid, J. R.; Nakamoto, K. *J. Am. Chem. Soc.* 1984, 106, 7741. (b) Kincaid, J. R.; Proniewicz, L. M.; Bajdor, K.; Bruha, A.; Nakamoto, K. *J. Am. Chem. Soc.* 1985, 107, 6775. (c) Proniewicz, L. M.; Nakamoto, K.; Kincaid, J. R. *J. Am. Chem. Soc.* 1988, 110, 4541. (d) Bruha, A.; Kincaid, J. R. *J. Am. Chem. Soc.* 1988, 110, 6006. (e) Proniewicz, L. M.; Bruha, A.; Nakamoto, K.; Kyuno, E.; Kincaid, J. R. *J. Am. Chem. Soc.* 1989, 111, 7050. (f) Proniewicz, L. M.; Kincaid, J. R. *J. Am. Chem. Soc.* 1990, 112, 675.

Clearly, the existence of such coupling effects would complicate the vibrational spectra of these O<sub>2</sub> adducts and compromise structural interpretations. It is thus important to elucidate the structural and electronic factors which influence such coupling interactions. For example, in a recent study of the O<sub>2</sub> adducts of cobalt porphyrins complexed with imidazole, it was demonstrated that hydrogen bonding of the coordinated imidazole has no effect on the strength of cobalt-oxygen bonding but does alter the vibrational coupling interactions to the extent that remarkable changes in the RR spectra are observed.<sup>5e,f</sup>

In the present work we focus on the issue of axial ligand disposition using two bis-strapped porphyrins in an attempt to induce distortion of the trans-axial ligand. The cobalt complexes of three superstructured "jellyfish" porphyrins,<sup>6</sup> 5α,15α-bis-[2-(2,2-dimethylpropanamido)phenyl]-10α,20α-(nonanediamidodi-*o*-phenylene)porphyrin (CoAz2-pivαα), 5β,15β:10α,20α-bis(nonanediamidodi-*o*-phenylene)porphyrin (CoAz2), and 5β,15β:10α,20α-bis(dodecanediamidodi-*o*-phenylene)porphyrin (CoDe2) (Figure 1), are used along with those of the simple, unstrapped, cobalt tetraphenylporphine (CoTPP). The resulting RR spectra reveal a distortion of trans-axial ligand binding in the case of CoAz2 (but not CoDe2) and demonstrate the utility of RR spectroscopy for probing subtle perturbations in axial ligand disposition.

## Experimental Section

**Compound Preparation.** 5,10,15,20-Tetraphenylporphine (H<sub>2</sub>TPP) was purchased from Midcentury Chemical Co. (Posen, IL) and purified to remove traces of reduced porphyrin by refluxing with 2,3-dichloro-5,6-dicyano-1,4-benzoquinone (DDQ) in toluene, extracting with sodium dithionite, and then chromatographing over dry alumina with chloroform.<sup>7</sup> β-Pyrrole deuterated H<sub>2</sub>TPP-*d*<sub>8</sub> was synthesized from the condensation reaction of pyrrole-*d*<sub>5</sub> and benzaldehyde in propionic acid-*d*<sub>8</sub><sup>8</sup> and purified as described above. "Jellyfish" porphyrins (5α,15α-bis-[2-(2,2-dimethylpropanamido)phenyl]-10α,20α-(nonanediamidodi-*o*-phenylene)porphyrin (H<sub>2</sub>Az2-pivαα), 5β,15β:10α,20α-bis(nonanediamidodi-*o*-phenylene)porphyrin (H<sub>2</sub>Az2), and 5β,15β:10α,20α-bis(dodecanediamidodi-*o*-phenylene)porphyrin (H<sub>2</sub>De2)) were prepared according to the methods described previously.<sup>6</sup> The β-pyrrole deuterated H<sub>2</sub>Az2-*d*<sub>8</sub> was prepared by using the same procedure as for H<sub>2</sub>Az2 but replacing pyrrole and acetic acid by their deuteriated analogues (pyrrole-*d*<sub>5</sub> and acetic acid-*d*<sub>4</sub>) as starting materials.

(6) Uemori, Y.; Miyakawa, H.; Kyuno, E. *Inorg. Chem.* 1988, 27, 377.

(7) Rousseau, K.; Dolphin, D. *Tetrahedron Lett.* 1974, 48, 4251.

(8) Adler, A. D.; Longo, F.; Finarelli, J. D.; Goldmacher, J.; Assour, J.; Korsakoff, L. *J. Org. Chem.* 1967, 32, 476.

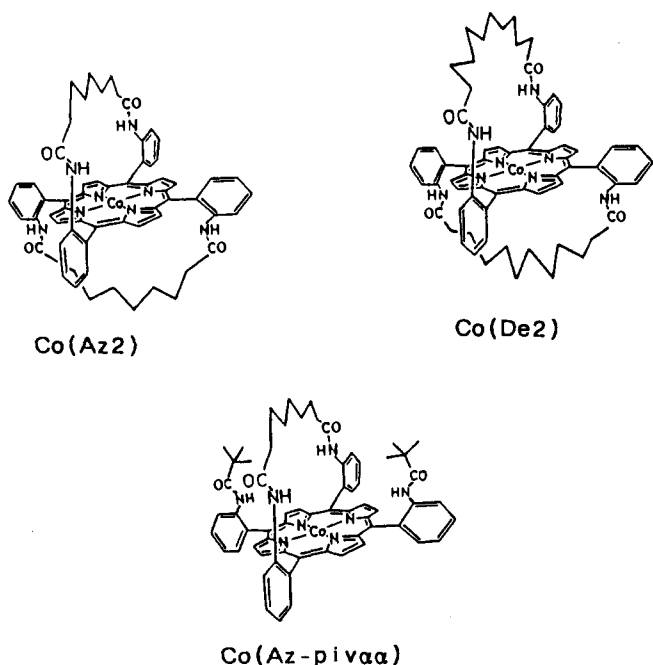


**Figure 1.** Structures of Co(Az2), Co(De2), and Co(Az-piv $\alpha\alpha$ ).

The iron was incorporated into H<sub>2</sub>TPP by refluxing the porphyrin in glacial acetic acid containing ferrous chloride.<sup>9</sup> Fe(TPP)(pip)<sub>2</sub> (pip = piperidine) was synthesized by reduction of Fe(TPP)Cl with piperidine in refluxing chloroform under a nitrogen atmosphere.<sup>10</sup> This compound was used as the starting material for Fe(TPP)(3,5-lutidine)<sub>2</sub> preparation (see Spectral Measurements section).

Cobalt was incorporated into H<sub>2</sub>TPP-*d*<sub>8</sub>, H<sub>2</sub>Az2, H<sub>2</sub>Az2-*d*<sub>8</sub>, and H<sub>2</sub>De2 by the reaction of cobaltous acetate with the porphyrin in refluxing chloroform while CoAz-piv $\alpha\alpha$  was prepared by reaction of cobaltous chloride with the porphyrin in refluxing dry tetrahydrofuran (THF) in the presence of 2,6-lutidine.<sup>6,11</sup> Reactions were carried out under a nitrogen atmosphere. Cobalt complexes were purified by chromatography on an alumina column according to a reported procedure.<sup>11</sup>

All bases were purchased from Aldrich Chemical Co. Pyridine (py), pyridine-*d*<sub>5</sub> (py-*d*<sub>5</sub>), and 3,5-lutidine (3,5-lut) were vacuum distilled over sodium hydroxide. Imidazole (Im) was purified by sublimation prior to deuteration. 2-Deuteroimidazole (Im-*d*<sub>1</sub>), 4,5-dideuteroimidazole (Im-*d*<sub>2</sub>), and 2,4,5-trideuteroimidazole (Im-*d*<sub>3</sub>) were synthesized as described previously<sup>5a</sup> and sublimed prior to sample preparation for RR measurements.

The solvents methylene chloride (CH<sub>2</sub>Cl<sub>2</sub>) and its deuterated analogue (CD<sub>2</sub>Cl<sub>2</sub>) and deuterated toluene (tol-*d*<sub>8</sub>) were purchased from Aldrich Chemical Co. CH<sub>2</sub>Cl<sub>2</sub> was purified by refluxing over calcium hydride and then distilled. Toluene-*d*<sub>8</sub> was used as supplied.

The gases <sup>16</sup>O<sub>2</sub> (greater than 99%, AmeriGas) and <sup>18</sup>O<sub>2</sub> (97% isotopic purity, ICON) were used without further purification.

**Spectral Measurements.** Spectral measurements were carried out by using the "minibulb" technique.<sup>12</sup> Dioxygen adducts of cobalt porphyrins were prepared following well-documented procedures.<sup>5a,c,e,13</sup> Fe(TPP)(3,5-lut)<sub>2</sub> was prepared by heating Fe(TPP)(pip)<sub>2</sub> in a minibulb at 200 °C for 2 h under vacuum of 10<sup>-3</sup> Torr to dissociate piperidine, followed by distillation of 3,5-lutidine. Next, dry and degassed CH<sub>2</sub>Cl<sub>2</sub> was transferred to dissolve the iron complex and the sample was prepared according to the "minibulb" preparation procedure.<sup>5a</sup>

The RR spectra were recorded on a Spex Model 1403 double monochromator equipped with a Hamamatsu R928 photomultiplier tube and a Spex DM1B computer. Excitations at 406.7 and 476.5 nm were accomplished with a Coherent Model 1100-K3 krypton ion laser and a Spectra Physics Model 2025 argon ion laser, respectively. Power at the sample was between 5 and 15 mW. A spectral band-pass of 4 cm<sup>-1</sup> was

(9) Chang, C. K.; DiNello, R. R.; Dolphin, D. In *Inorganic Synthesis*; Busch, D. H., Ed.; Wiley: New York, 1981; Vol. 20, p 157.

(10) Epstein, L. M.; Straub, D. K.; Maricondi, C. *Inorg. Chem.* 1967, 6, 1720.

(11) Collman, J. P.; Braumann, J. I.; Doxsee, K. M.; Halbert, T.; Hayes, S. E.; Suslick, K. S. *J. Am. Chem. Soc.* 1978, 100, 2761.

(12) Nakamoto, K.; Nonaka, Y.; Ishiguro, T.; Urban, M. W.; Suzuki, M.; Kozuka, M.; Nishida, Y.; Kida, S. *J. Am. Chem. Soc.* 1982, 104, 3386.

(13) Proniewicz, L. M.; Odo, J.; Goral, J.; Chang, C. K.; Nakamoto, K. *J. Am. Chem. Soc.* 1989, 111, 2105.

### Co(TPP-*d*<sub>8</sub>)(py)(O<sub>2</sub>) in CH<sub>2</sub>Cl<sub>2</sub>

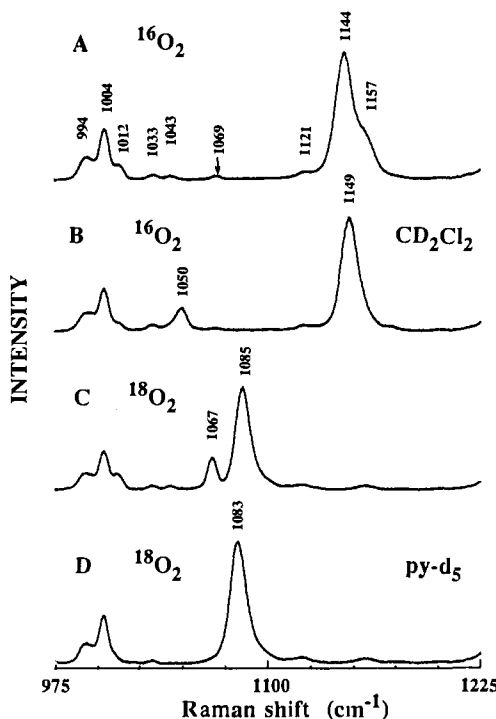


**Figure 2.** Resonance Raman spectra of O<sub>2</sub> adducts of Co(TPP-*d*<sub>8</sub>) complexes with pyridine in CH<sub>2</sub>Cl<sub>2</sub> (excitation at 406.7 nm): (A) <sup>16</sup>O<sub>2</sub>; (B) <sup>16</sup>O<sub>2</sub>, CD<sub>2</sub>Cl<sub>2</sub>; (C) <sup>18</sup>O<sub>2</sub>; (D) <sup>18</sup>O<sub>2</sub>, py-*d*<sub>5</sub>.

routinely used. Accuracy of the frequency readings was  $\pm 1$  cm<sup>-1</sup>. A CTI Model 21 closed-cycle helium cryocooler was used to maintain samples at the desired temperature during the measurements.

### Results and Discussion

**A. O<sub>2</sub> Adducts of Pyridine Complexes. 1. Unhindered Ligation.** The RR spectra of the O<sub>2</sub> adducts of the pyridine complex of Co(TPP-*d*<sub>8</sub>), a reference compound which imposes no steric restrictions on binding of the trans-axial pyridine ligand, are shown in Figure 2. The <sup>16</sup>O<sub>2</sub> adduct in CH<sub>2</sub>Cl<sub>2</sub> (trace A) exhibits a strong feature at 1144 cm<sup>-1</sup> with a pronounced shoulder at 1157 cm<sup>-1</sup>. In this case, the  $\nu(^{16}\text{O}-^{16}\text{O})$  is coupled with an internal mode (1156 cm<sup>-1</sup>) of an intimately associated solvent molecule.<sup>5a</sup> This interpretation is confirmed by the fact that the  $\nu(^{16}\text{O}-^{16}\text{O})$  is observed at 1149 cm<sup>-1</sup> when CD<sub>2</sub>Cl<sub>2</sub> is used as the solvent (trace B).

Given an inherent  $\nu(^{16}\text{O}-^{16}\text{O})$  frequency of 1149 cm<sup>-1</sup>, a simple harmonic oscillator approximation yields an expected  $\nu(^{18}\text{O}-^{18}\text{O})$  at  $\sim 1083$  cm<sup>-1</sup>. As is shown in trace C, however, a weak satellite line is observed at 1067 cm<sup>-1</sup> along with the strong feature at 1085 cm<sup>-1</sup>. This weak feature is an internal mode of the trans-axial pyridine ligand which gains intensity as a consequence of vibrational coupling with the  $\nu(^{18}\text{O}-^{18}\text{O})$ . Again, the existence of such coupling is confirmed by the fact that upon replacement of pyridine with pyridine-*d*<sub>5</sub> (which has no internal modes in this region), the inherent frequency of  $\nu(^{18}\text{O}-^{18}\text{O})$  is revealed as the expected frequency of 1083 cm<sup>-1</sup> as shown in trace D (i.e.,  $\Delta\nu = +2$  cm<sup>-1</sup>). This implies that the inherent frequency of the bound pyridine is 1069 cm<sup>-1</sup> (i.e., 2 cm<sup>-1</sup> above the 1067 cm<sup>-1</sup> of the coupled mode). A very weak feature observed at 1069 cm<sup>-1</sup> in the spectrum of the <sup>16</sup>O<sub>2</sub> adduct (trace A) together with bands at 1012 and 1043 cm<sup>-1</sup> is due to a metal-to-ligand charge transfer (MLCT) which enhances modes of coordinated pyridine.<sup>14</sup> Thus, the spectra shown in Figure 2 demonstrate that a sterically unrestricted

(14) (a) Spiro, T. G.; Burke, J. M. *J. Am. Chem. Soc.* 1976, 98, 5482. (b) Burke, J. M.; Kincaid, J. R.; Peters, R. R.; Gagne, J. P.; Collman, J. P.; Spiro, T. G. *J. Am. Chem. Soc.* 1978, 100, 6083. (c) Wright, P. G.; Stein, P.; Burke, J. M.; Spiro, T. G. *J. Am. Chem. Soc.* 1979, 101, 3531. (d) Schick, G. A.; Bocian, D. F. *J. Am. Chem. Soc.* 1984, 106, 1682.

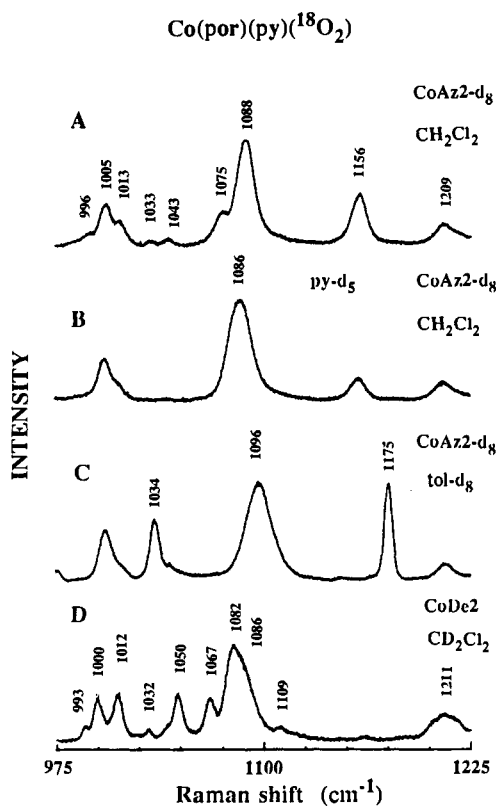


**Figure 3.** Resonance Raman spectra of  $^{18}\text{O}_2$  adducts of Co(por)(py) complexes (excitation at 406.7 nm): (A) CoAz2- $d_8$ ,  $\text{CH}_2\text{Cl}_2$ ; (B) CoAz2- $d_8$ ,  $\text{CH}_2\text{Cl}_2$ ; (C) CoAz2- $d_8$ , tol- $d_8$ ; (D) CoDe2,  $\text{CD}_2\text{Cl}_2$ .

ligated pyridine possesses an internal mode at  $1069\text{ cm}^{-1}$  which may vibrationally couple with  $\nu(\text{O}-\text{O})$ . In the case of the  $^{16}\text{O}_2$  adduct, the inherent frequencies are sufficiently remote so as to prevent detectable frequency perturbations. On the other hand, the proximity of  $\nu(^{18}\text{O}-^{18}\text{O})$  to the  $1069\text{-cm}^{-1}$  mode gives rise to more efficient coupling, leading to frequency perturbations of  $\pm 2\text{ cm}^{-1}$ , behavior which is consistent with existing theory.<sup>5f,15</sup>

**2. Strapped Porphyrins.** The RR spectra of the  $\text{O}_2$  adducts of the pyridine complexes with CoAz2 and CoDe2 are given in Figure 3. Inasmuch as the relevant pyridine internal mode is efficiently coupled with  $\nu(^{18}\text{O}-^{18}\text{O})$ , it is only necessary to investigate the  $^{18}\text{O}_2$  adducts. As can be seen by comparison of traces A and B, an internal pyridine mode is observed at  $1075\text{ cm}^{-1}$  (trace A). The inherent frequency of the  $\nu(^{18}\text{O}-^{18}\text{O})$  is revealed at  $1086\text{ cm}^{-1}$  (trace B) where pyridine- $d_5$  is utilized. The  $-2\text{ cm}^{-1}$  shift of the strong feature upon removal of the coupling implies that the inherent frequency of the internal pyridine mode is  $1077\text{ cm}^{-1}$ , i.e., its frequency is lowered in trace A by  $2\text{ cm}^{-1}$  as a consequence of coupling with  $\nu(^{18}\text{O}-^{18}\text{O})$ . Thus, by comparison of Figure 2C with Figure 3A, it is clear that the presence of the strap in the complex with CoAz2 imposes an encumbrance to trans-axial ligand binding which, in turn, induces a  $+8\text{ cm}^{-1}$  ( $1075-1067\text{ cm}^{-1}$ ) frequency perturbation of the internal mode of the bound pyridine.

In the absence of further investigation, it could be argued that the pyridine band at  $1077\text{ cm}^{-1}$  does not correspond to the  $1069\text{-cm}^{-1}$  feature. Specifically, free pyridine possesses two modes at around  $1070\text{ cm}^{-1}$  which are assigned to an in-plane CCH bending,  $\beta(\text{CCH})$  vibrations.<sup>16</sup> One, which has  $A_1$  symmetry (Wilson number 18a), is observed at  $1068\text{ cm}^{-1}$ . The second, of  $B_1$  symmetry (Wilson number 18b), is expected to occur near the

same frequency ( $1074\text{ cm}^{-1}$ ).<sup>15a</sup> According to Mulliken's convention,<sup>17</sup> the  $B_1$  modes reported in refs 15a and 15b become the  $B_2$  modes. Although the 18b mode is non-totally symmetric in the case of free pyridine, it is possible that symmetry lowering with the bound complex could yield a depolarization ratio of less than  $3/4$  (the measured value is  $1/3$ ). However, we have eliminated this possibility by employing pyridine-4-*d* whereupon essentially the same spectrum as that shown in trace A of Figure 3 was obtained.<sup>18</sup> On the basis of previously reported data, the 18b mode (but not the 18a mode) experiences a large downshift (about  $100-150\text{ cm}^{-1}$ ) in monodeuteriopyridines.<sup>16</sup> Since such a shift was not observed, we conclude that the  $1069\text{-cm}^{-1}$  band corresponds to 18a.

In addition to the  $8\text{-cm}^{-1}$  upshift induced by the steric constraints of the strap, we also note a detectable weakening in the strength of vibrational coupling. Thus, as is shown in trace C of Figure 3, when toluene- $d_8$  is used as the solvent, no satellite feature is observed in this region. The solvent-induced shift of  $\nu(^{18}\text{O}-^{18}\text{O})$  from  $1086\text{ cm}^{-1}$  (trace B) to  $1096\text{ cm}^{-1}$  (trace C) is comparable to that observed for analogous (unprotected) CoTPP adducts<sup>5b</sup> and implies that the strap does not impede interaction of  $\text{CH}_2\text{Cl}_2$  with the bound dioxygen. The essential point here is that, in the case of CoAz2, the bound pyridine is apparently sufficiently distorted to weaken vibrational coupling to such an extent that the two modes ( $1077$  (py) and  $1096\text{ cm}^{-1}$ ) are non-interacting; whereas in the case of unrestrained pyridine bonding coupling is observed between the  $1067$  (py) and  $1094\text{ cm}^{-1}$  modes of CoTPP(py) $^{18}\text{O}_2$  in toluene.<sup>5b</sup>

The  $8\text{-cm}^{-1}$  upshift of the pyridine mode is apparently caused by the steric hindrance between the strap and pyridine molecule that, in turn, influences the  $\beta(\text{CCH})$  vibrations. In "unprotected" metalloporphyrins, such as CoTPP, the axial ligand is perpendicular to the mean porphyrin plane and tends to take the eclipsed orientation with respect to the N-Co-N axis.<sup>19</sup> Model building studies indicate that, in the case of the 9-carbon atom polymethylene strap (CoAz2), pyridine is too large to fit into the cavity.

While the pyridine plane can assume either a parallel or perpendicular orientation relative to the strap, the rotation of the pyridine relative to the porphyrin plane is inhibited by the strap in either case. In addition, both the strap and the pyridine may deviate from the plane perpendicular to the mean porphyrin plane. Somewhat surprisingly, such a distorted orientation of pyridine does not significantly influence the strength of the cobalt-oxygen linkage. This is based on the observation that the  $\nu(\text{Co}-\text{O}_2)$  and  $\nu(\text{O}-\text{O})$  exhibit inherent frequencies quite similar to the dioxygen adducts obtained with (unencumbered) Co( $T_{\text{piv}}\text{PP}$ ).<sup>5b</sup>

It is interesting to note that this apparent axial ligand distortion is relaxed in the case of the  $\text{O}_2$  adducts with CoDe2, which possesses a longer, more flexible strap. Thus, as is shown in trace D of Figure 3, the  $\nu(^{18}\text{O}-^{18}\text{O})$  is observed at  $1086\text{ cm}^{-1}$  as a shoulder overlapped with the  $1082\text{-cm}^{-1}$  porphyrin band and the internal pyridine mode again appears at its normal frequency of  $1067\text{ cm}^{-1}$  (inherent frequency of  $1069\text{ cm}^{-1}$ ). The strong feature observed at  $1082\text{ cm}^{-1}$  is associated with an internal mode of the CoDe2. Apparently, in the case of CoAz2, the relatively short strap length induces a distortion of the bound pyridine, whereas the more flexible strap of CoDe2 permits unrestrained axial ligand binding. The effect of the distortion induced by the short strap is to alter the frequencies of the internal modes of the bound ligand and to weaken the strength of vibrational coupling with  $\nu(\text{O}-\text{O})$ .

Steric hindrance between the strap and the axial ligand also influences other physicochemical properties of metalloporphyrins. For example, Kyuno et al.<sup>6,20</sup> reported that the equilibrium constant ( $K_B$ ) values for pyridine or 1-methylimidazole (1-MeIM) binding to CoAz2 complex are about 100-fold less than those for CoDe2 or CoAz-piv $\alpha\alpha$  complexes and pointed out that the binding of pyridine or 1-MeIM is inhibited selectively in the case of CoAz2 porphyrin. Also, Desbois et al.<sup>21</sup> noted that iron(II) complexes

(15) (a) Fermi, E. Z. *Phys.* 1931, 71, 250. (b) Herzberg, G. *Molecular Spectra and Structure*; Van Nostrand: New York, 1945; Vol. 2, p 215. (c) Veas, C.; McHale, J. L. *J. Am. Chem. Soc.* 1989, 111, 7042.

(16) (a) Sverdlov, L. M.; Kovner, M. A.; Krainov, E. P. In *Vibrational Spectra of Polyatomic Molecules*; Halsted Press: New York, 1974; p 522. (b) Dollish, F. R.; Fateley, W. G.; Bently, F. F. *Characteristic Raman Frequencies of Organic Compounds*; Wiley: New York, 1974. (c) DiLella, D. P.; Stidham, H. D. *J. Raman Spectrosc.* 1980, 9, 90.

(17) Mulliken, R. S. *J. Chem. Phys.* 1955, 23, 1997.

(18) Proniewicz, L. M.; Bajdor, K.; Golus, J. In preparation.

(19) Scheidt, W. R.; Chipman, D. M. *J. Am. Chem. Soc.* 1986, 108, 1163.

(20) Uemori, Y.; Kyuno, E. *Inorg. Chim. Acta* 1986, 125, L45.

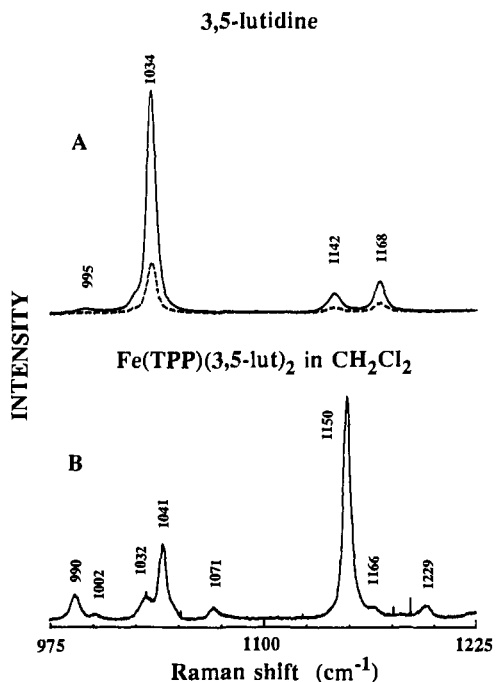


**Figure 4.** (A) Raman spectra of pure 3,5-lutidine excited at 476.5 nm. The dotted line represents the spectrum taken with perpendicular polarization. (B) Resonance Raman spectrum of Fe(TPP)(3,5-lutidine)<sub>2</sub> in CH<sub>2</sub>Cl<sub>2</sub> with excitation at 476.5 nm.

of [bis(picket)(9-carbon atom polymethylene strap)]TPP, when reacted with 1-MeIm, formed mainly a 5-coordinate complex. Apparently, the bulky pickets and a short strap restrict the axial ligand binding inside the porphyrin "pocket". Thus, 1-MeIm binds preferentially from the "unprotected" side of the porphyrin plane. When the 9-carbon atom strap is replaced by a 12-carbon atom strap (CoDe2), a 6-coordinate complex (Fe(por)(1-MeIm)<sub>2</sub>) is formed; i.e., the size of the cavity is large enough to accommodate the axial ligand. They<sup>21</sup> also reported that the  $\nu(\text{Fe}-\text{O}_2)$  is practically insensitive to the strap length, a result which is consistent with our data.

**B. O<sub>2</sub> Adducts of 3,5-Lutidine Complexes.** In an attempt to amplify the strap-induced distortion of the trans-axial ligand we have employed a pyridine analogue of greater steric bulk, namely, 3,5-lutidine. The Raman spectrum of free 3,5-lutidine (lut) in the region of interest is given in Figure 4A. Two lines at 1168 and 1142 cm<sup>-1</sup> are observed in the  $\nu(\text{O}^{16}\text{O}-\text{O}^{18}\text{O})$  region, but no Raman active modes occur in the  $\nu(\text{O}^{18}\text{O}-\text{O}^{18}\text{O})$  region ( $\sim 1085$  cm<sup>-1</sup>). Trace B gives the spectrum of the bis-lutidine complex with FeTPP obtained in resonance with a metal-to-ligand charge transfer (MLCT) transition which efficiently enhances internal modes of coordinated lutidine. Similar MLCT enhancement was reported previously for coordinated pyridine.<sup>14</sup> This spectrum exhibits a strong internal mode of coordinated lutidine occurring at 1150 cm<sup>-1</sup> with a weak shoulder at 1166 cm<sup>-1</sup>. The weak feature at 1071 cm<sup>-1</sup> is an internal mode of the (non-deuteriated) TPP macrocycle.

**1. Unhindered Ligation.** Figure 5 shows the RR spectra of the O<sub>2</sub> adducts of the CoTPP-d<sub>8</sub> complex with 3,5-lutidine under various conditions. In trace A, the  $\nu(\text{O}^{18}\text{O}-\text{O}^{18}\text{O})$  is observed as a strong isolated (uncoupled) feature at 1081 cm<sup>-1</sup> which yields an expected frequency for  $\nu(\text{O}^{16}\text{O}-\text{O}^{18}\text{O})$  at 1147 cm<sup>-1</sup>. As is shown in trace B, however, the  $\text{O}^{16}\text{O}$  adduct exhibits two relatively strong features at 1160 and 1138 cm<sup>-1</sup>. The appearance of this doublet is clearly ascribable to coupling of the  $\nu(\text{O}^{16}\text{O}-\text{O}^{18}\text{O})$  (inherent frequency of 1147 cm<sup>-1</sup>) with the internal mode of coordinated 3,5-lutidine at 1150 cm<sup>-1</sup> (Figure 4A). Thus, the stronger 1138-cm<sup>-1</sup> component, which contains a larger contribution from  $\nu(\text{O}^{16}\text{O}-\text{O}^{18}\text{O})$ , is shifted 9 cm<sup>-1</sup> below its inherent value of 1147 cm<sup>-1</sup>.

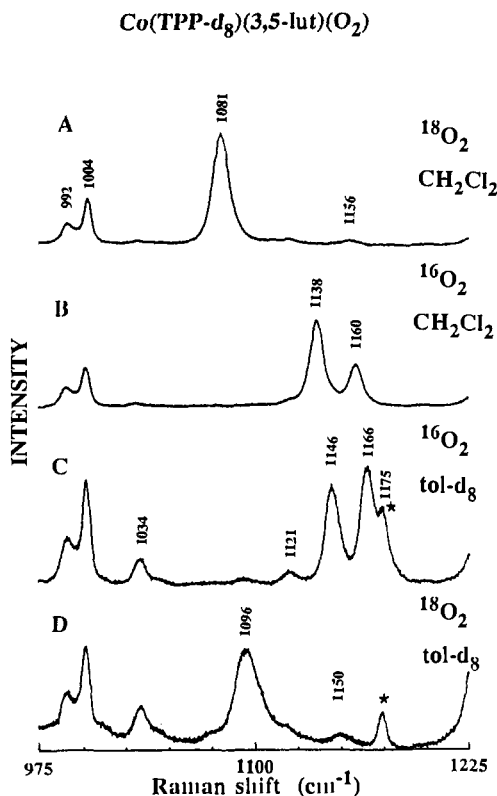


**Figure 5.** Resonance Raman spectra of O<sub>2</sub> adducts of Co(TPP-d<sub>8</sub>)(3,5-lut) complexes (excitation at 406.7 nm): (A) <sup>18</sup>O<sub>2</sub>, CH<sub>2</sub>Cl<sub>2</sub>; (B) <sup>16</sup>O<sub>2</sub>, CH<sub>2</sub>Cl<sub>2</sub>; (C) <sup>16</sup>O<sub>2</sub>, tol-d<sub>8</sub>; (D) <sup>18</sup>O<sub>2</sub>, tol-d<sub>8</sub>. The asterisk indicates the toluene-d<sub>8</sub> band.

while the weaker, higher frequency, mode is shifted 9–10 cm<sup>-1</sup> above its inherent frequency of 1150 cm<sup>-1</sup> (Figure 4A).

Traces C and D of Figure 5 demonstrate that such coupling persists in toluene-d<sub>8</sub>. Thus, given an inherent  $\nu(\text{O}^{18}\text{O}-\text{O}^{18}\text{O})$  of 1096 cm<sup>-1</sup> (trace D), the inherent frequency of  $\nu(\text{O}^{16}\text{O}-\text{O}^{16}\text{O})$  is expected to be 1162 cm<sup>-1</sup> ( $\Delta\nu = +66$  cm<sup>-1</sup>). Coupling of  $\nu(\text{O}^{16}\text{O}-\text{O}^{16}\text{O})$  with the 1150-cm<sup>-1</sup> lutidine mode gives rise to two components shifted  $\pm 4$  cm<sup>-1</sup> from their inherent frequencies (i.e., 1150 → 1146 cm<sup>-1</sup> and 1162 → 1166 cm<sup>-1</sup>).

It is worthwhile to point out that the relative intensities of the coupled modes in trace B (1138 and 1160 cm<sup>-1</sup>) and trace C (1166 and 1146 cm<sup>-1</sup>) are qualitatively consistent with the "expected behavior".<sup>5f</sup> Thus, in the case of CH<sub>2</sub>Cl<sub>2</sub>, the inherent  $\nu(\text{O}^{16}\text{O}-\text{O}^{16}\text{O})$  (1147 cm<sup>-1</sup>) occurs at a lower frequency than the 1150-cm<sup>-1</sup> lutidine mode and the lower frequency component of the coupled modes exhibits the greater intensity. On the other hand, in the case of toluene-d<sub>8</sub>, the inherent  $\nu(\text{O}^{16}\text{O}-\text{O}^{16}\text{O})$  (1162 cm<sup>-1</sup>) occurs at a higher frequency than the 1150-cm<sup>-1</sup> ligand mode and the 1166-cm<sup>-1</sup> component is stronger than the 1146-cm<sup>-1</sup> feature.

**2. Strapped Porphyrins.** The RR spectra of the O<sub>2</sub> adducts of 3,5-lutidine complexes with superstructured porphyrins are given in Figure 6. The occurrence of the  $\nu(\text{O}^{18}\text{O}-\text{O}^{18}\text{O})$  at 1095 cm<sup>-1</sup> in trace A leads to an expected  $\nu(\text{O}^{16}\text{O}-\text{O}^{18}\text{O})$  of 1161 cm<sup>-1</sup> (i.e.,  $\Delta\nu = +66$  cm<sup>-1</sup>). As can be seen in trace B, the  $\nu(\text{O}^{16}\text{O}-\text{O}^{18}\text{O})$  appears at precisely this frequency, indicating a complete absence of coupling with the internal lutidine mode which occurs in this region. Presumably, the greater distortion experienced by the sterically more demanding lutidine (relative to pyridine) is sufficient to effectively eliminate coupling of the internal modes. Again, as in the case of the pyridine complexes (Figure 3D), the greater flexibility of the longer strap of CoDe2 apparently facilitates unencumbered ligand binding and permits efficient coupling of the modes so as to produce two relatively strong features at 1142 and 1161 cm<sup>-1</sup> (trace C). The 8 cm<sup>-1</sup> lowering of the lutidine mode from 1150 to 1142 cm<sup>-1</sup> implies that the inherent frequency of  $\nu(\text{O}^{16}\text{O}-\text{O}^{18}\text{O})$  is 1153 cm<sup>-1</sup> (i.e., 8 cm<sup>-1</sup> lower than the observed frequency at 1161 cm<sup>-1</sup>).

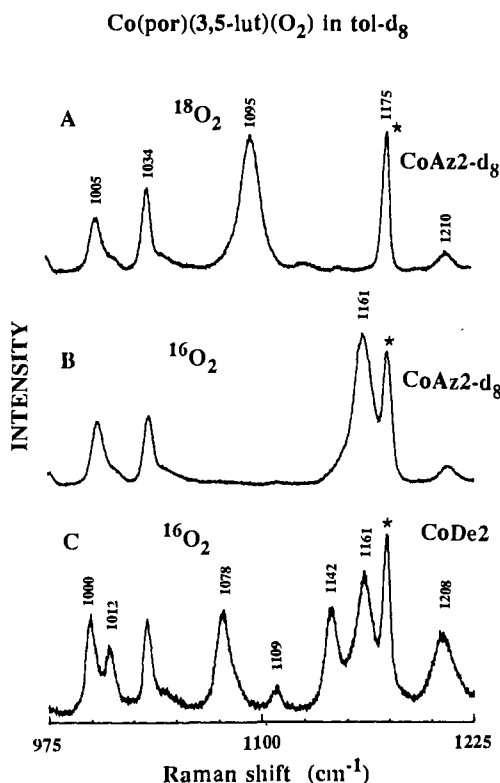


**Figure 6.** Resonance Raman spectra of  $O_2$  adducts of  $\text{Co}(\text{por})(3,5\text{-lut})$  complexes in toluene- $d_8$  (excitation at 406.7 nm): (A)  $^{18}\text{O}_2$ ,  $\text{CoAz2-}d_8$ ; (B)  $^{16}\text{O}_2$ ,  $\text{CoAz2-}d_8$ ; (C)  $^{16}\text{O}_2$ ,  $\text{CoDe2}$ . The asterisk indicates the toluene- $d_8$  band.

**C.  $O_2$  Adducts of Imidazole Complexes.** In our earlier work,<sup>5e</sup> it was demonstrated that the  $O_2$  adducts of cobalt-porphyrin complexes with imidazole experience efficient vibrational coupling of  $\nu(\text{O}-\text{O})$  with internal modes of the trans-axial imidazole. Strategic isotopic labeling studies, employing isotopomers of dioxygen as well as selectively deuterated imidazoles, permitted identification of specific internal modes of the various imidazole isotopomers.<sup>5f</sup> In the present study, we utilize this information to investigate the effects of steric encumbrance on the RR spectra of these species.

Inasmuch as  $\nu(^{16}\text{O}-^{16}\text{O})$  had been found to efficiently couple with imidazole modes in the 1120–1150- $\text{cm}^{-1}$  region,<sup>5e</sup> we have focused attention on the  $^{16}\text{O}_2$  adducts in the present study. The RR spectra, in the region of interest, of all complexes studied are given in Figure 7. The previously reported spectra of the (sterically unrestricted)  $\text{CoAz-piv}\alpha\alpha$  adducts with  $^{16}\text{O}_2$  are reproduced here for comparison purposes.

In the case of natural abundance imidazole, the  $\nu(^{16}\text{O}-^{16}\text{O})$ , having an inherent frequency of 1144  $\text{cm}^{-1}$ , couples with an internal imidazole mode (inherent frequency of 1153  $\text{cm}^{-1}$ ) to give rise to two components observed at 1138 and 1158  $\text{cm}^{-1}$  (i.e.,  $\Delta\nu = 6 \text{ cm}^{-1}$ ). As can be seen in Figure 7, this coupling is effectively eliminated in the case of the  $\text{CoAz2}$  complex, a behavior which is consistent with the results obtained with 3,5-lutidine and pyridine. Also, as in the case of these latter complexes, such coupling is again efficient in the case of the  $\text{CoDe2}$  analogue. Similar results are obtained for the imidazole- $d_1$  complex which possesses an internal mode at 1150  $\text{cm}^{-1}$ ; i.e., coupling in the cases of  $\text{CoAz-piv}\alpha\alpha$  and  $\text{CoDe2}$  gives rise to two components shifted by approximately 7  $\text{cm}^{-1}$  from their inherent frequencies.

In the cases of the complexes with  $\text{Im-}d_2$  and  $\text{Im-}d_3$ , the  $\text{CoAz2}$  analogues exhibit coupled modes with components at 1134 and 1148  $\text{cm}^{-1}$ . Assuming an inherent frequency of  $\nu(^{16}\text{O}-^{16}\text{O})$  of 1141  $\text{cm}^{-1}$  (from data for the  $\text{Im}$  and  $\text{Im-}d_1$  complexes), the interacting imidazole modes apparently possess an inherent frequency of 1140  $\text{cm}^{-1}$  for both  $\text{Im-}d_2$  and  $\text{Im-}d_3$ . Thus, an internal imidazole mode of this frequency couples with the  $\nu(^{16}\text{O}-^{16}\text{O})$ , giving rise to two components whose frequencies are shifted by 7  $\text{cm}^{-1}$  from their

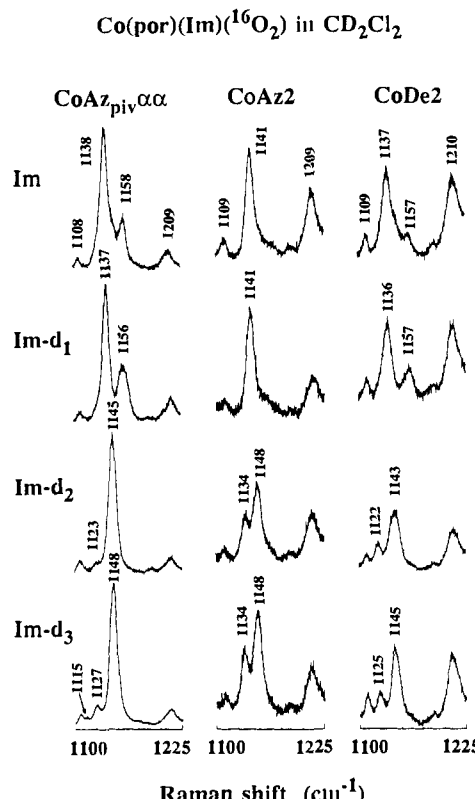


**Figure 7.** Resonance Raman spectra of  $^{16}\text{O}_2$  adducts of  $\text{Co}(\text{por})$  complexes with imidazole and its deuteriated analogues in  $\text{CD}_2\text{Cl}_2$  (excitation at 406.7 nm).

inherent (nearly accidentally degenerate) frequencies. Comparison of the three complexes with  $\text{Im-}d_2$  indicates that steric strain associated with the short strap of  $\text{CoAz2}$  induces a distortion which results in an 18- $\text{cm}^{-1}$  shift to higher frequency; i.e., the  $\sim 1122\text{-cm}^{-1}$  mode observed in the cases of  $\text{CoAz-piv}\alpha\alpha$  and  $\text{CoDe2}$  occurs at  $\sim 1140 \text{ cm}^{-1}$  in the case of  $\text{CoAz2}$ .

The behavior observed for the imidazole complexes closely parallels that observed for the pyridine case. Thus, the short strap of  $\text{CoAz2}$  induces shifts of the  $1069\text{-cm}^{-1}$  (pyr),  $1122\text{-cm}^{-1}$  ( $\text{Im-}d_2$ ), and  $1125\text{-cm}^{-1}$  ( $\text{Im-}d_3$ ) modes to higher frequency (by 8–18  $\text{cm}^{-1}$ ) and considerably weakens the strength of vibrational coupling.

**D. Implications for RR Studies of Heme Proteins.** The results of the present study reinforce our previously reported results and conclusion<sup>5c–f</sup> that carefully conducted RR studies of the dioxygen adducts of cobalt-substituted heme proteins can provide a direct probe of proximal histidyl-imidazole disposition, but for static and transient (using time-resolved RR techniques) species. Such information, which is not readily attainable by other methods (especially for transient species), has considerable value for elucidating the effect of axial ligand disposition on heme reactivity and protein control mechanisms.

#### Summary Conclusions

The relatively short strap length of the  $\text{CoAz2}$  complex causes distortion of the trans-axial ligand, while the longer, more flexible, strap of the  $\text{CoDe2}$  analogue permits unrestrained binding. While the strength of the  $\text{Co-O}_2$  linkage remains relatively unaltered by this distortion (the inherent  $\nu(\text{O}-\text{O})$  and  $\nu(\text{Co}-\text{O}_2)$  frequencies are not substantially changed), the ligand internal modes are perturbed and result in detectable spectral differences. This study clearly demonstrates that RR spectroscopy is quite useful for detecting subtle steric-induced perturbations of axial ligand disposition in these important model compounds.

**Acknowledgment.** L.M.P. expresses his gratitude for Grant WCH-30/91 provided to the Jagiellonian University by the Polish Ministry of Education. This work was supported by grants from the National Institutes of Health (DK 35153 to J.R.K.) and the National Science Foundation (DMB-8613741 to K.N.).